

Reaction Mechanism of Various Types of Lunar Soil Simulants by Hydrogen Reduction

Katsuya Sueyoshi, Takayuki Watanabe*, Yoshio Nakano
Dept. Environmental Chemistry and Engineering, Tokyo Institute of Technology
4259 Nagatsuta, Midori-ku, Yokohama, Kanagawa 226-8502, Japan
*watanabe@chemenv.titech.ac.jp

Hiroshi Kanamori, Shigeru Aoki
Shimizu Corporation, Institute of Technology
3-4-17 Etchujima, Koto-ku, Tokyo 135-8530, Japan

Akira Miyahara, Kai Matsui
Japan Aerospace Exploration Agency, Institute of Space and Astronautical Science
2-1-1 Sengen, Tsukuba, Ibaraki, 305-8505, Japan

Abstract

Several processes to produce water and oxygen from lunar regolith have been proposed. Among these processes, hydrogen reduction process of lunar regolith has several advantages. Therefore, we have investigated the water-production mechanism by H_2 reduction for three types of lunar soil simulants. The maximum of water-production was obtained for all lunar soil simulants at 1323 K. Mössbauer spectra of FJS-1 revealed that the produced water was generated from ilmenite, Fe^{3+} phase(s), and magnetic materials such as hematite or magnetite. The cross-section observation of scanning electron microscope and BET method presented that the surface area was decreased at higher temperature owing to melting of some components in the cracks, and the surface area was increased as the progress of hydrogen reduction. The kinetic consideration using thermogravimetry indicated that hydrogen reduction for lunar soil was controlled by chemical reaction.

1. Introduction

Lunar exploration projects are advancing to a more active phase. For future lunar and planetary sustainable exploration and development, in-situ resource utilization (ISRU) technology will be much more important for the engineering purposes. ISRU technology will require the use of locally derived materials since transportation from the earth requires much time, cost, and labor. ISRU will provide production of water, oxygen, helium-3, metals, and other materials. In these materials, water and oxygen are the most important in early human exploration phase. Two methods are considered to produce water as stated below.

One of the conceivable lunar water-production methods is to utilize lunar water ice that might exist at the lunar poles. However, it has not been revealed yet if sufficient quantities of lunar ice exist or not.

Another method to produce water is reduction of lunar soil by H_2 as shown in Fig. 1. This process consists of two of the most feasible processes that are the reduction of ilmenite in lunar soil and the reduction of ferrous iron in volcanic glass (Taylor and Carrier, 1992). For this reason, several researchers have studied the reduction of ilmenite and volcanic glass. Zhao and Shadman (1991) investigated H_2 reduction mechanism of ilmenite powder (less than 45 μm) prepared by cold press molding. The reaction followed a shrinking core model and consists of five primary steps. Kapilashrami *et al*. (1996) investigated the reaction mechanism by thermogravimetric method for synthetic ilmenite which particle size was about 150 μm. They concluded that ilmenite ($FeTiO_3$) was reduced to TiO_2 and iron below 1186 K, but at and above

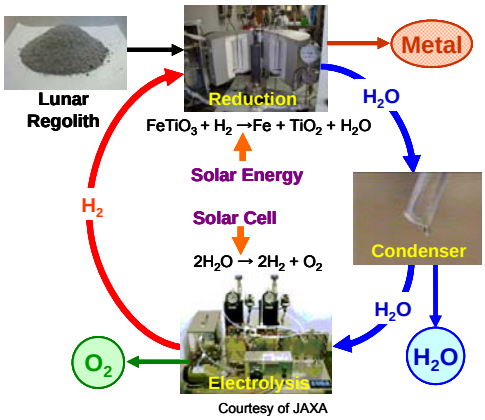

Figure 1. Schematic diagram of H_2 reduction system.

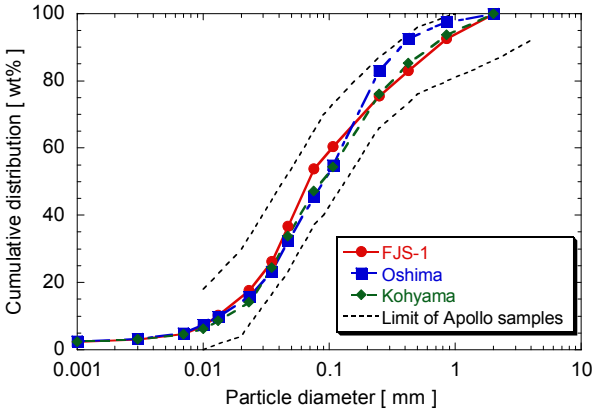

Figure 2. Particle diameter distribution of lunar soil simulants.

this temperature the reduction products were found to be Ti_3O_5 and iron (Kapilashrami, 1996). Olivine, pyroxene, and other main components included in lunar soil also have been studied. Allen *et al*. (1996, 1994) have conducted experiments on various lunar soils and glass samples. Olivine and pyroxene contained in lunar soils and glasses were partially reduced. Massieon *et al*. (1993) have studied the kinetics and mechanisms of the reduction of olivine by H_2. The solid products after reduction were iron and vitreous silica, and the products formed a nanoporous layer around an unreacted core. They described that permeation of H_2 through this nonporous layer was important in determining the rate of reduction.

Investigations of the reaction mechanism of lunar soil by H_2 reduction are not enough for ISRU development though water-production methods on the moon have been studied by many researchers. Therefore, the purpose of this research is to investigate the reduction mechanism of water-production by H_2 reduction of three types of lunar soil simulants that have different chemical types. Understanding of the H_2 reduction mechanism of different types of lunar soil simulants is important for the mission of utilizing the lunar soil because chemical components of lunar soil depend on the site.

2. Samples and Methods

2.1. Samples

Three types of lunar soil simulants were used for experiments. Lunar soil simulants were produced by Shimizu Corp., Japan. Fuji lava base (FJS-1), Oshima lava base (Oshima), and Kohyama gabbro base (Kohyama) mimic low-Ti mare, high-Ti mare, and intermediate of mare and highland lunar regolith, respectively. Chemical components for three types of simulants except for oxygen are shown in Table 1. FJS-1 and Kohyama are made of basalt in Mt. Fuji, Japan, and gabbro in Kohyama, in Japan, respectively. Oshima made of basalt containing volcanic glass with addition of 7wt%-forsterite and 8wt%-ilmenite to mimic the chemical components of lunar regolith in high-Ti mare. Figure 2 shows that each simulant has similar particle distributions to mimic lunar regolith, and that average diameters (Martin diameters) of FJS-1, Oshima and Kohyama are 67, 88, 85 μm, respectively.

2.2. Experimental apparatus for water-production

A fixed-bed reactor was used for water-production experiments. The details of

Elements	Si	Ti	Al	Cr	Fe^{2+}	Fe^{3+}	Mn	Mg	Ca	Na	K	P	S	Total
FJS-1	38.87	1.74	16.75	0.04	5.83	11.47	0.39	4.13	14.24	4.81	1.43	0.30	0.01	100.00
Oshima	36.31	5.81	11.71	0.08	8.17	14.42	0.49	7.42	12.15	2.71	0.64	0.08	0.01	100.00
Kohyama	44.39	0.70	18.05	0.05	3.52	9.04	0.24	2.97	15.25	4.13	1.52	0.13	0.01	100.00

Table 1. Chemical components of lunar soil simulants.

experimental set-up were reported by Watanabe *et al*. (2006). Sample weight was 5 g on this experiment.

Experiment was started by first flowing He at 0.50 NL/min for sample heating up to reduction temperature and preventing from oxidation. After 20 min, He was quickly switched to H_2 at 4.00 NL/min. The inlet pressure was kept at 202 kPa by controlling back pressure valve. Both gases flew up through a preheating gap between the inner and the outer tubes. H_2 with produced water was transported to moisture meter to measure the water-production rate.

2.3. Sample morphology

The morphology of initial, heated, and H_2 reduced lunar soil simulants was analyzed. FJS-1 mounted in an epoxy resin and polished to expose the cross section of the grain was observed with scanning electron microscope (SEM) to investigate the particle structural change by H_2 reduction. The specific surface area (SSA) and pore volume distribution were measured by BET using N_2 and Kr as adsorption gas. Iron Mössbauer spectroscopy (FeMS) was used to analyze the iron morphology.

2.4. TG analysis

The weight reduction of the simulant by H_2 reduction was measured using thermogravimetry (TG) to investigate the reaction kinetics. Sample weight of FJS-1 or Oshima in alumina crucible was 50 mg, while that of Kohyama was 100 mg because of Kohyama contains little iron-bearing minerals than the others. Heating rate was 100 K/min in He atmosphere. H_2 reduction was started after reaching prescribed temperature and then holding the temperature for about 20 min. H_2 flow rate was 0.020 NL/min with 0.48 NL/min He flow.

3. Results and Discussion

3.1. Water-production

The effect of reduction temperature on the water-production rate and cumulative amount is important to investigate the reaction mechanism of lunar soil simulants. Effect of reduction temperature on the water-production rate by the fixed-bed reactor system is shown in Fig. 3. Higher temperature gave higher water-production rate up to 1273 K. H_2 reduction rate of FJS-1 is fairly high in the experimental temperature range. The peak-top positions are found within 0.5 min and the most of water-production terminated after about 5 min.

Figure 4 shows effect of reduction temperature on the cumulative amount of water-production for all simulants. The amount of water-production was evaluated at the complete reduction. Increase of cumulative amount of water production for FJS-1 and Kohyama is slight. In contrast, that for Oshima is significant with temperature up

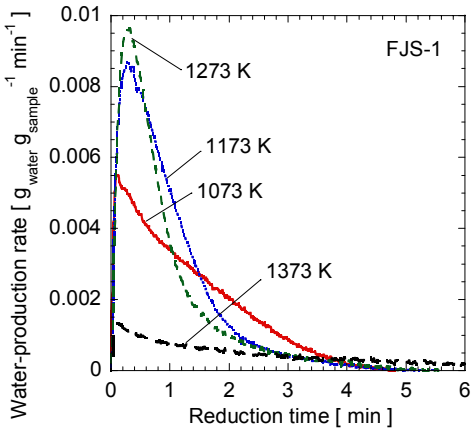

Figure 3. Effect of reduction temperature on water-production rate by a fixed-bed reaction reactor.

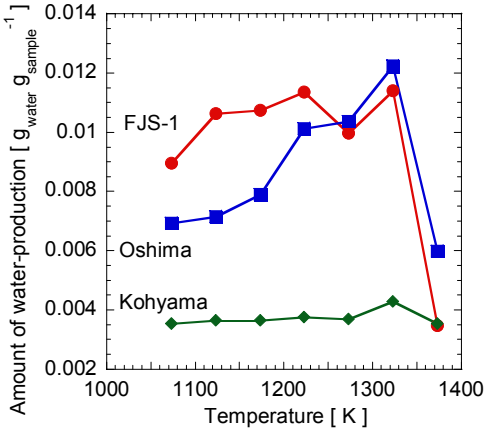

Figure 4. Effect of reduction temperature on the amount of water-production by a fixed-bed reaction reactor.

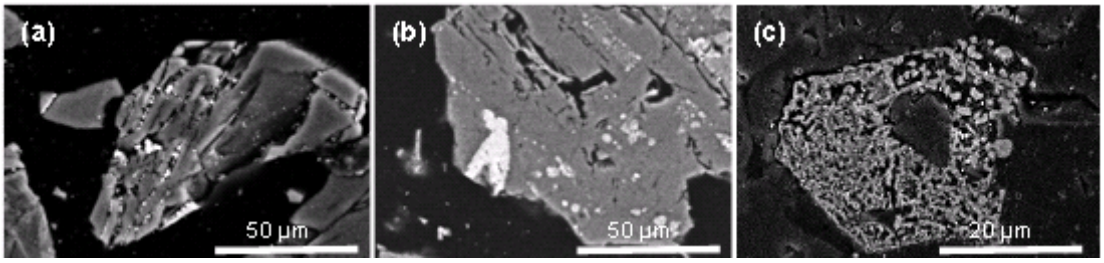

Figure 5. Cross-section of FJS-1. (a): Raw material, (b): Heated to 1273 K, (c): Reduced at 1273 K by H_2.

to 1323 K owing to reduction of volcanic glass, because the total amount of glass reduction is strongly temperature dependent (Allen *et al.*, 1994). At 1373 K, the cumulative amount of water-production for all simulants sharply decreased because of melting of some components in simulants. The water-production amount from FJS-1 was higher than that from Oshima, even though Oshima contains richer iron fractions than FJS-1. From this result, the water-production amount cannot be directly correlated to the iron fractions in the initial sample.

3.2. Sample morphology

3.2.1. SEM observation

The cross-section observation of FJS-1 was conducted to investigate the morphology change on heating and H_2 reduction. The results of SEM observations are shown in Fig. 5. Higher atomic number components generate stronger intensity of backscattered electrons, thereby the regions which have larger atomic number show a lighter-colored image (Taylor *et al.*, 1996). The brightest regions in the particles are ilmenite-like minerals.

The particles have several cracks containing fine particles as the SEM image of Fig. 5(a). In contrast, the cracks of heated samples contain few fine particles as shown in Fig. 5(b). These SEM results mean that the fine particles were molten, and then fine particles might be integrated into large particles and transformed into a number of roundish blobs.

The ilmenite-like regions, as shown in Fig. 5(c), have a myriad of holes after reduction because oxygen atoms were extracted by H_2 reduction. The generation of holes were evaluated from the pore volume distribution measured by BET method.

3.2.2. Results of BET methods

The SSA was decreased by heating and was increased by H_2 reduction for all simulants as shown in Fig. 6. N_2 was used as the adsorbent for raw material, besides

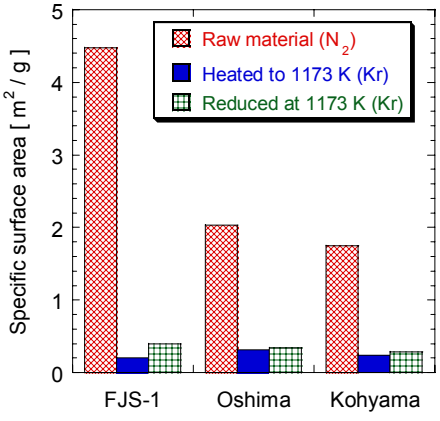

Figure 6. SSA for lunar soil simulants. The adsorption gas for raw material is N_2 and that for heated and reduced products is Kr.

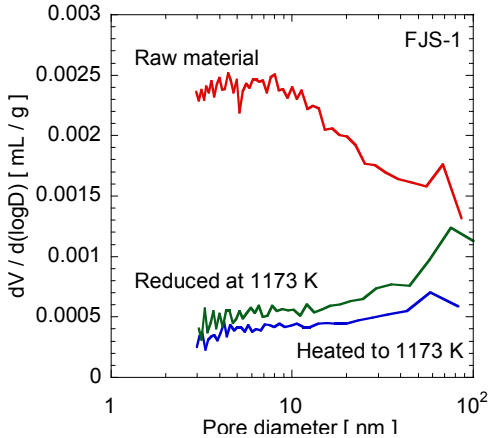

Figure 7. Pore volume distribution change of FJS-1 influenced on heating and H_2 reduction. The adsorption gas for all samples is N_2. V: Pore volume, D: Pore diameter.

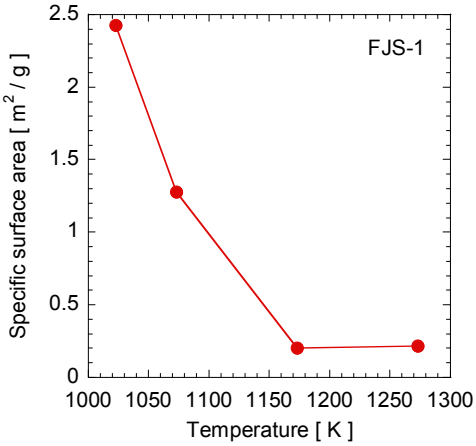

Figure 8. Effect of heating temperature on SSA for FJS-1.

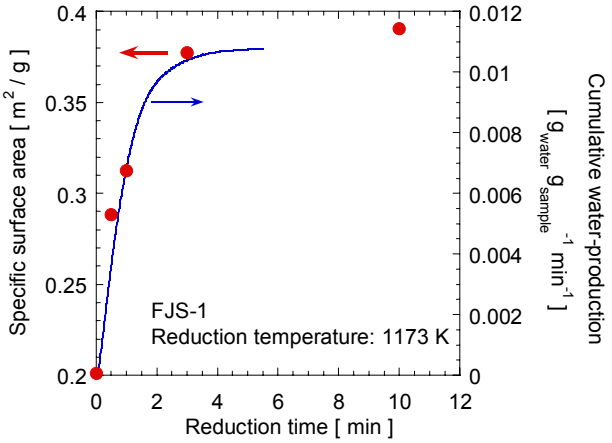

Figure 9. Increasing of SSA and cumulative water-production with time for FJS-1.

Kr was used for the heated and reduced samples because both samples have relatively small SSA (<1 m^2/g). Measurement by Kr adsorption leads to more exact results than that by N_2. The results from SEM images and BET measurements indicate that the molten fine particles made SSA lower, and H_2 reduction increased SSA. Figure 7 shows the pore volume distribution of initial, heated, and reduced FJS-1. The contribution of smaller pore diameter was decreased by heating. In contrast, the contribution of larger pore diameter was increased by H_2 reduction.

The effect of heating temperature on the SSA for FJS-1 is shown in Fig. 8. Higher temperature gives smaller SSA up to 1173 K. This result indicates higher temperature lead to increase of the amount of molten components.

The increases of SSA and of cumulative water-production with reduction time for FJS-1 by the fixed-bed reactor system are shown in Fig. 9. The SSA was increased with the cumulative water-production. This indicates that the SSA was increased with the water-production by H_2 reduction. As stated above, H_2 reduction of FJS-1 made a myriad of holes. These results indicate that increasing SSA is attributed to oxygen extraction by H_2.

3.2.3. Results of FeMS

Iron-bearing minerals in the lunar soil simulants were analyzed by FeMS because the water-production rate and cumulative amount cannot be correlated to the fraction of iron oxide as stated above. Mössbauer spectra of FJS-1 are shown in Fig. 10. Several researchers have reported the Mössbauer spectra of olivine basalt (Gunnlaugsson *et al.*, 2006) and lunar soil (Allen *et al.*, 1996, 1994; Gibson *et al.*, 1994). Iron-bearing minerals for our experimental data by FeMS were identified by these references. The quantity of each iron-bearing mineral of the lunar soil simulants, in particular, the fraction of area spectra of pyroxene, olivine, ilmenite, Fe^{3+} phase(s), and two sextet magnetic minerals was shown in Table 2. Fe^{3+} is the most likely origin of pyroxene (Gunnlaugsson *et al.*, 2006). Magnetic materials were regarded as iron oxides such as hematite, maghemite, or magnetite. These iron oxides can easily be reduced by H_2 in the temperature range of our experiments. Pyroxene, olivine, α-Fe and γ-Fe spectra are contained in the reduced FJS-1. The area fractions of pyroxene and olivine for FJS-1 differ little from that of after reduction. This directly indicates that pyroxene and olivine are unreducible at 1173 K, but that the other iron-bearing minerals are reducible by H_2.

3.3. TG analysis of reaction kinetics

TG analysis was conducted to discuss the reaction kinetics of H_2 reduction for lunar soil. Ilmenite and iron oxides in the lunar soil simulants are mainly reducible minerals by H_2 from the results of FeMS. Weight loss derives from the reduction of these components. Figure 11 shows the effect of reduction temperature on the cumulative

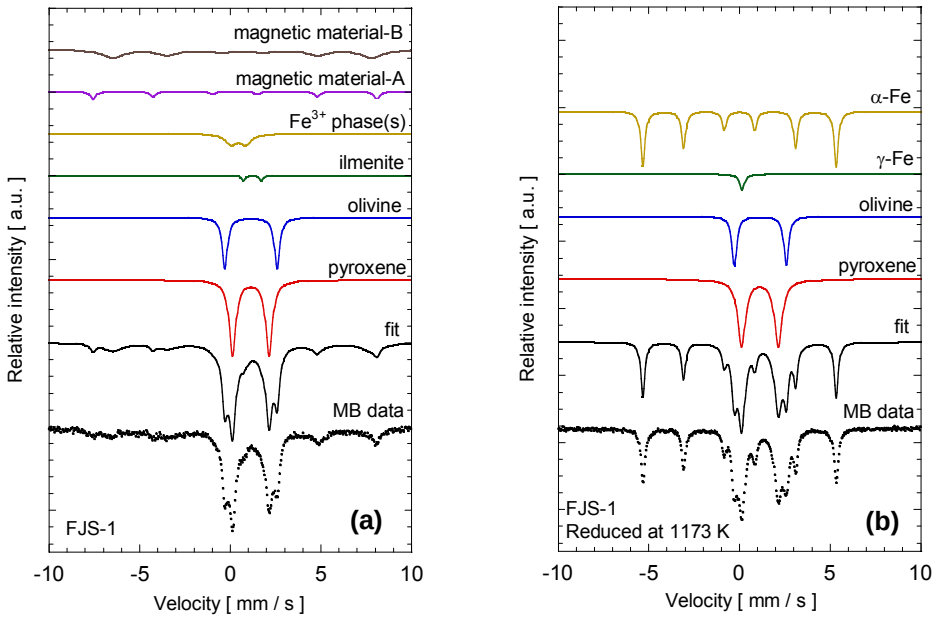

Figure 10. Mössbauer spectra of FJS-1. MB data: Mössbauer data of samples, fit: Sum of the identified components.

Sample	Identification	IS [mm/s]	QS [mm/s]	B_{hf} [T]	Area [%]
FJS-1	pyroxene	1.14	2.02		38.1
	olivine	1.14	2.88		20.6
	ilmenite	1.22	0.97		1.5
	Fe^{3+} phase(s)	0.45	0.82		8.7
	magnetic material-A	0.26		48.6	5.9
	magnetic material-B	0.67		44.3	25.3
FJS-1 (reduced)	pyroxene	1.13	2.03		41.8
	olivine	1.15	2.87		18.9
	γ-Fe	0.14			3.0
	α-Fe	0.00		33.1	36.3

Table 2. Hyperfine parameters derived from Mössbauer spectra of FJS-1. IS: The isomer shift, QS: The quadrupole splitting, B_{hf}: The internal magnetic field.

weight loss due to H_2 reduction and conversion ratio of FJS-1 by TG. Conversion ratio x was defined as follows:

$$x = \frac{\text{Cumulative weight loss}}{\text{Oxygen weight bonding with iron}} \quad (1)$$

The denominator was calculated with Table 1 regarding Fe^{2+} and Fe^{3+} as FeO and Fe_2O_3, respectively. The numerator could be obtained from TG. Conversion ratio of unity means that oxygen has completely extracted from iron.

Conversion ratio reached approximately 0.31 at most. The conversion ratio less than unity is attributed to the unreducible iron-bearing minerals such as pyroxene and olivine contained in FJS-1 as shown in Table 2.

The effect of reduction temperature on the water-production rate by TG is shown in Fig. 12. The maximum value of water-production rate increases with temperature. The peak-top is located in conversion ratio of 0.15-0.20 at 1155 and 1251 K, but the position is found at conversion ratio of 0.025 at 1298 K. This result indicates the molten components filled up pores at 1298 K and the components inhibited H_2 diffusion into the pores of FJS-1. Therefore, at 1298 K, reduction took longer time than the others as shown in Fig. 11.

The data obtained by TG analysis was applied to Arrhenius equation to estimate the

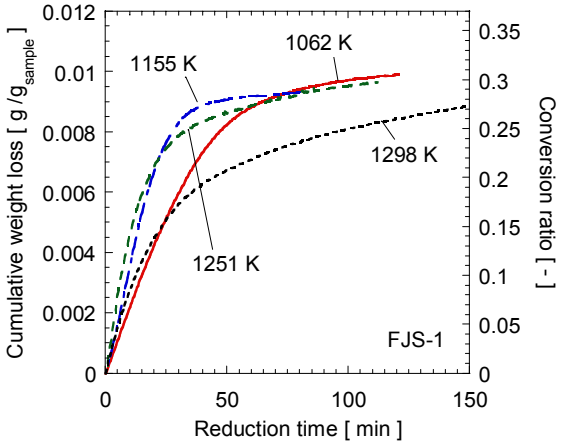

Figure 11. Effect of temperature on cumulative weight loss and conversion ratio of FJS-1 by TG.

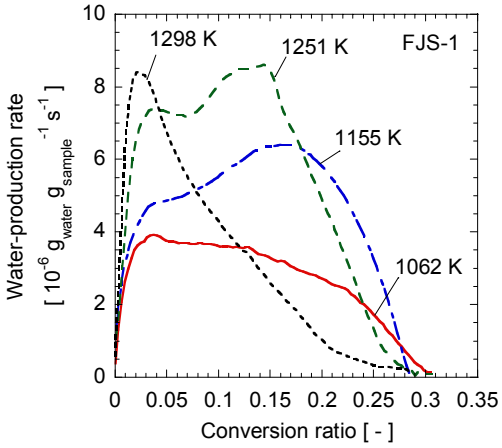

Figure 12. Effect of temperature on water-production rate of FJS-1 by TG.

activation energy and to investigate the reaction-controlling step. Arrhenius plot of FJS-1 was shown in Fig. 12. Reaction rate constant k was calculated by Eq. (2) with assumption of first-order reaction with respect to H_2 concentration.

$$k = \frac{r}{C_{H_2}} \tag{2}$$

where r is water-production rate and C_{H2} is H_2 concentration. The plots are on each straight line with respect to conversion ratio from 1062 K to 1201 K, but the plots are not on the straight lines at 1251 K and above. Activation energy for all simulants was calculated from the gradients of these linear regressions in Fig. 13 with Eq. (3).

$$\ln k = \ln A - \frac{E}{RT} \tag{3}$$

where A is frequency factor, R is gas constant, and E is activation energy. The estimated activation energies are shown in Fig. 14. The activation energy of 50-80 kJ/mol for FJS-1 was coincident with the intermediate value of iron oxides and ilmenite (e.g. Pitrowski *et al.*, 2007; Kapilashrami *et al.*, 1996; Briggs and Sacco 1990). The activation energy of Oshima and Kohyama increased with the reduction.

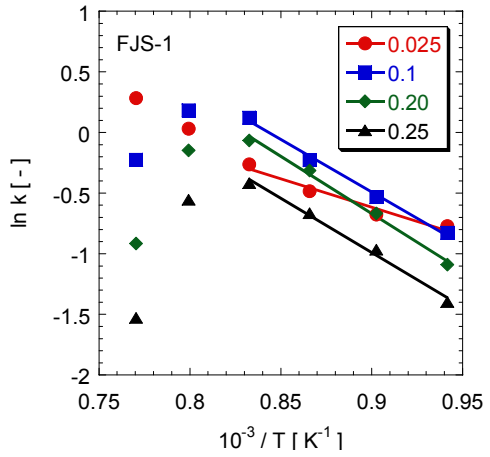

Figure 13. Arrhenius plot for H_2 reduction of FJS-1. The values in a graph legend are conversion ratio.

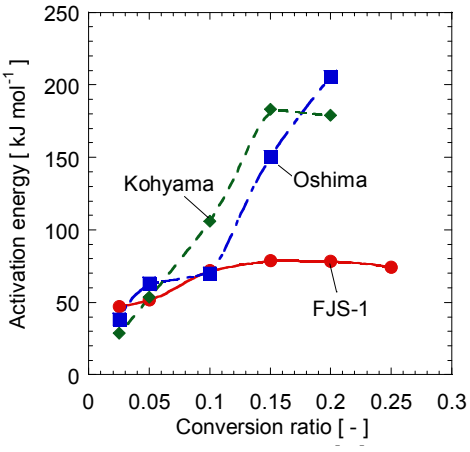

Figure 14. Activation energy for lunar soil simulants.

Besides, the values of Oshima and Kohyama (206 and 179 kJ/mol at conversion ratio of 0.2, respectively) are significantly higher than that of ilmenite and iron oxides. The reason is that Oshima contains abundant volcanic glass and Kohyama has poor iron minerals. The activation energy for glass reduction is over twice that for mare soil reduction over the temperature range 1173-1323 K (Allen *et al.*, 1994). Thus, the rate-controlling step of H_2 reduction for lunar soil simulants was the reaction step of reducible oxides.

4. Conclusions

Three types of lunar soil simulants were used for investigating the reaction mechanism of water-production by H_2 reduction of lunar soil.

The activation energy for FJS-1 was lower than that for Oshima and Kohyama owing to rich content of iron oxides in FJS-1, and the activation energy was the intermediate value of iron oxides and ilmenite. On the contrary, the activation energy of Oshima and Kohyama increased with the reduction because Oshima contains abundant volcanic glass and Kohyama has poor iron minerals.

Therefore, the rate-controlling step for lunar soil was the reaction step of reducible oxides with H_2.

References

Allen, C. C., R. V. Morris, and D. S. McKay (1996), "Oxygen extraction from lunar soils and pyroclastic glass," *J. Geophys.Res.*, **101**, 26,085-26,095.

Allen, C. C., R. V. Morris, and D.S. McKay (1994), "Experimental reduction of lunar mare soil and volcanic glass," *J. Geophys. Res.*, **99**, 23,173-23,185.

Briggs, R. A. and A. Sacco, Jr. (1990), "Hydrogen reduction mechanism of ilmenite between 823 and 1353 K," *J. Mater. Res.*, **6**(3), 574-584.

Gibson, M. A., C. W. Knudsen, D. J. Brueneman, C. A. Allen, H. Kanamori, and D. S. McKay (1994), "Reduction of lunar basalt 70035: Oxygen yield and reaction product analysis," *J. Geophys. Res.*, **99**, 10,887-10,897.

Gunnlaugsson, H. P., Ö. Helgason, L. Kristjánsson, P. Nørnberg, H. Rasmussen, S. Steinþórsson, and G. Weyer (2006), "Magnetic properties of olivine basalt: Application to Mars," *Phys. Earth Planet. Int.*, **154**, 276-289.

Kapilashrami, A., I. Arvanitidis, and Du Sichen (1996), "Investigation of the kinetics of reduction of iron titanate ($FeTiO_3$) by hydrogen," *High Temp. Mater., Process.*, **15**, 73-81.

Massieon, C. C., A. H. Cutler and F. Shadman (1993), "Hydrogen reduction of iron-bearing silicates," *Ind. Eng. Chem. Res.*, **32**, 1239-1244.

Piotrowski, K., K. Mondal, T. Wiltowski, P. Dydo and G. Rizeg (2007), "Topochemical approach of kinetics of the reduction of hematite to wüstite," *Chem. Eng. J.*, **131**, 73-82.

Taylor, L. A. and W. D. Carrier III (1992), "Production of oxygen on the moon: Which process are best and why," *AIAA J.*, **30**, 2858-2863.

Taylor, L. A., A. Patchen, D. W. S. Taylor, J. G. Chambers, and D. S. McKay (1996), "X-ray digital imaging petrography of lunar mare soils: Modal analyses of minerals and glasses," *Icarus*, **124**, 500-512.

Watanabe, T., S. Komatsuzaki, H. Kanamori, and S. Aoki (2006), "Kinetic investigation of water production from lunar soil simulant by hydrogen reduction," *Space Resources Roundtable VIII*, 66-67.

Zhao, Y. and F. Shadman (1991), "Reduction of ilmenite with hydrogen," *Ind. Eng. Chem. Res.*, **30**, 2080-2087.